Journal of Applied Geophysics 88 (2013) 1–11

Contents lists available at SciVerse ScienceDirect

Journal of Applied Geophysics

journal homepage: www.elsevier.com/locate/jappgeo

Surface deformation induced by water influx in the abandoned coal mines in Limburg, The Netherlands observed by satellite radar interferometry

Miguel Caro Cuenca, Andrew J. Hooper, Ramon F. Hanssen *

Dept. of Geoscience and Remote Sensing, Delft University of Technology, Delft, The Netherlands

ARTICLE INFO

Article history:
Received 19 April 2012
Accepted 7 October 2012
Available online 13 October 2012

Keywords:
InSAR
Persistent scatterers
Groundwater dynamics
Coal mine

ABSTRACT

The coal reserves of Limburg, The Netherlands, have been exploited until the mid-1970's, leading to significant land subsidence, a large part of which was due to ground water pumping associated with the mining activities. In 1994, when also the hydrologically-connected neighboring German mining activities ceased, all pumps were finally dismantled. This resulted in rising groundwater levels in the mining areas, continuing until today. Here we report the detection and analysis of heterogeneous surface displacements in the area using satellite radar interferometry. The lack of adequate terrestrial geodetic measurements emphasizes the value of such satellite observations, especially in terms of the temporal and spatial characterization of the signal. Since the lack of direct mine water level measurements hampers predictions on future consequences at the surface, we study the relationship between surface deformation and sub-surface water levels in an attempt to provide rough correlation estimates and map the mine water dynamics.

1. Introduction

The coal reserves of the southern Netherlands, see Fig. 1, were exploited for many centuries. Extraction at an industrial scale commenced in the beginning of the twentieth century and peaked between 1950 and 1975 (van Bergen et al., 2007). As exploitation became less economically interesting most of the Dutch mines closed during the seventies.

This long-term extraction resulted in land subsidence. The total subsidence that occurred since the beginning of 1900s is estimated to be in order of several meters (Pöttgens, 1985). Subsidence in mining areas occurred due to two different causes. First, the partial collapse of galleries after the actual extraction of coal reduced support of the upper layers producing surface deformation. Second, as the mining activities require a dry working space, groundwater was continuously pumped from the galleries and the rock layers surrounding them. The stress change due to coal extraction and pore pressure decrease produced by the pumping resulted in subsidence.

After the mines were abandoned and pumping halted, the groundwater flowed back to hydrostatic equilibrium producing the opposite effect — the land began to rise. Not anticipated at the time, first indications of uplift were observed for an incidental leveling line in 1978, four years after closure of the last mine (Pöttgens, personal communication, 2008). Pöttgens (1985) explained the uplift due to a pore pressure increase produced by the rising groundwater in the mines. To protect the neighboring German mines, still operational, from being flooded, the pump in the shaft of Beerenbosch II, near the German border, Fig. 2, remained active. Furthermore, a system of subsurface water barriers (dams) was installed by sealing most of the galleries interconnecting the mine concessions (Bekendam and Pöttgens, 1995), which were originally built as evacuation corridors for safety reasons (Wings, personal communication, 2011). However, some of the galleries were left open to control groundwater flow.

As a consequence, the coal fields were divided into a series of so-called *water basins* formed from the original concessions, which were usually delimited by natural faults. The water basins had overflowing corridors that connected them to the only remaining pump in the field, located in Beerenbosch II, i.e. southern basin. This pump was eventually disabled early 1994 (Bekendam and Pöttgens, 1995). The cease of the pumping in this year led to a rapid increase in the groundwater level in the southern basin. During 1994, the groundwater level rose from −215 m to −138 m NAP[1] and started to overflow towards the central basin. The profile A–A' in Fig. 2 shows the overflowing levels and the groundwater regime at the time when the pump in Beerenbosch II was active, (Bekendam and Pöttgens, 1995). Currently, the groundwater is still flowing back into the concession areas, bounded by the dam system (Rosner, 2011; Wings, 2006). Consequently, groundwater recharge is not synchronous throughout the region and is expected to produce a deformation pattern that changes in place and time.

* Corresponding author.
E-mail addresses: m.carocuenca@tudelft.nl (M. Caro Cuenca), a.j.hooper@tudelft.nl (A.J. Hooper), r.f.hanssen@tudelft.nl (R.F. Hanssen).

[1] NAP (Normaal Amsterdams Peil) is the vertical Dutch datum. The local topography ranges from 50 to 200 m NAP.

0926-9851/$ – see front matter © 2012 Elsevier B.V. All rights reserved.
http://dx.doi.org/10.1016/j.jappgeo.2012.10.003

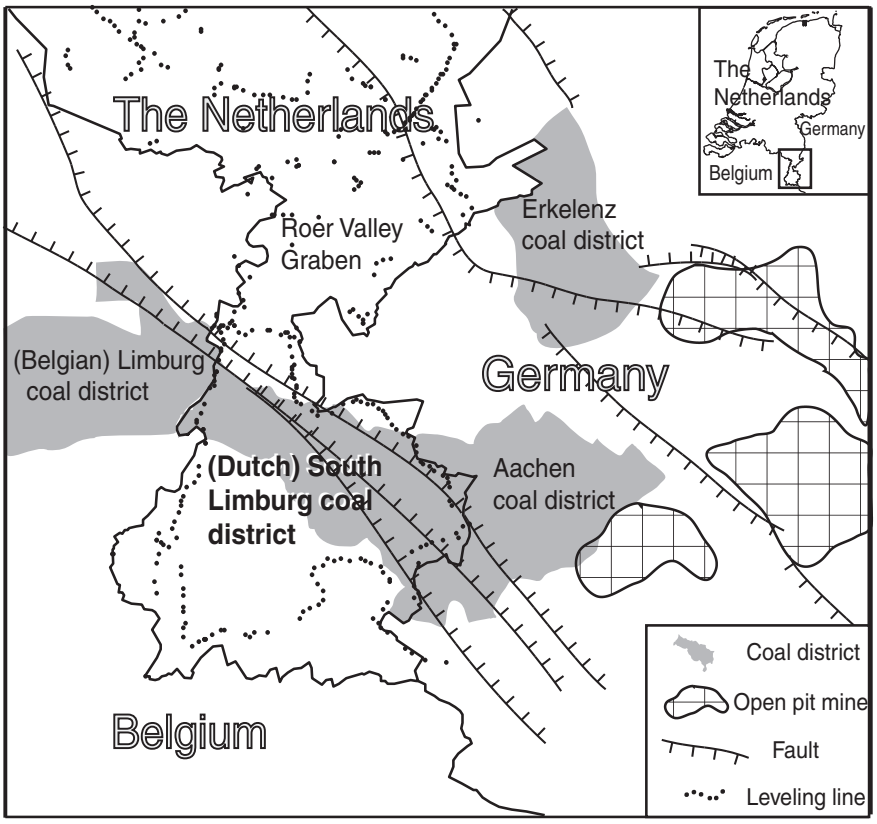

Fig. 1. Coal fields in the southern Netherlands and adjacent regions, after (Devleeschouwer et al. (2008), Heitfeld et al. (2002) and TNO (1999)). German open pit lignite mines are also shown, as water pumping in these areas influences the surface motion. Reliable leveling benchmarks that were measured at least three times during the period 1992–2009 are also displayed.

Until now, the mines have been monitored mostly with leveling. Unfortunately, to study the whole deformation process with this technique is difficult because leveling campaigns are rather limited in extent, spatially sparse and have a low measurement frequency, see Fig. 1.

In depth comprehension of mine water dynamics can also help to predict hazardous situations derived from mine water flow and consequent surface motion, such as building or pipe damage. In the German city of Wassenberg, near Limburg, the cessation of pumping in abandoned mines led to infrastructure damage, nine buildings were reported to be strongly affected (Caro Cuenca and Hanssen, 2011; Heitfeld et al., 2006). Satellite-based radar measurements provide a spatio-temporally dense network of observations that can be used to aid the analysis of such complex deformation mechanisms. In contrast to conventional Synthetic Aperture Radar Interferometry, (InSAR), which estimates deformation and height from two images acquired at different times (Hanssen, 2001), persistent scatterer interferometry (PSI) utilizes a time series of spaceborne radar acquisitions to identify objects whose scattering properties remain stable over time. The pixels representing these objects are electromagnetically coherent and referred to as persistent scatterers (PS). The phase information obtained from their radar returns can be reliably used to infer surface deformation time series (Ferretti et al., 2001; Hooper et al., 2004; Kampes, 2006). Most PS are related to anthropogenic constructions, with a common density about 100 PS per km^2 in urban environments for the C-band sensors (ERS1/2 and Envisat). The detection and use of coherent scatterers aids phase unwrapping (unfolding the phase outside its natural range of $(-\pi,\pi]$) and the estimation of atmospheric signals, which are the dominant error sources when estimating surface deformation.

We employ PSI to measure surface displacements in the Dutch coal region, potentially subject to mine water recharge. The total study area is 50×45 km^2. The deformation time series is obtained with the Delft implementation of PSI (DePSI), with the unwrapping algorithm of Caro Cuenca et al. (2010) where the solutions of most stable PS are used to constrain and weigh the solution space of the rest of detected PS using Bayesian inference. The interferograms are created with the Doris software (Kampes et al., 2003).

Two data sets are used in this study. The first one was acquired by the ERS1/2 satellites between April 1992 and December 2000, yielding 74 radar images. The second set includes 59 images provided by the Envisat satellite and acquired from December 2003 to October 2009. Satellite precise orbits are provided by the Delft University of Technology, (Scharroo and Visser, 1998), and by ESA (European Space Agency).

In Section 2, we apply PSI to the mines in Limburg and report cumulative displacements and time series analysis. We estimate total displacements and describe the spatio-temporal behavior of the signal in Section 3, by analyzing how the deformation changes in time and space. We model the volume increase suffered by the mines from the total surface displacements in Section 4.

2. Surface displacements observed by PSI

We processed almost 18 years of radar acquisitions to produce line of sight (LOS) displacement time series. We projected the LOS direction to vertical assuming vertical-only displacements. The whole time span was initially divided into two stacks as provided by the European satellites ERS1/2 and Envisat. These two sets of displacement time series were low pass filtered in time and space to reduce noise. The time series were merged to produce longer time series from April 1992 to October 2009 (Caro Cuenca and Hanssen, 2010). The procedure to join time series assumes that the displacements in ERS1/2 and Envisat

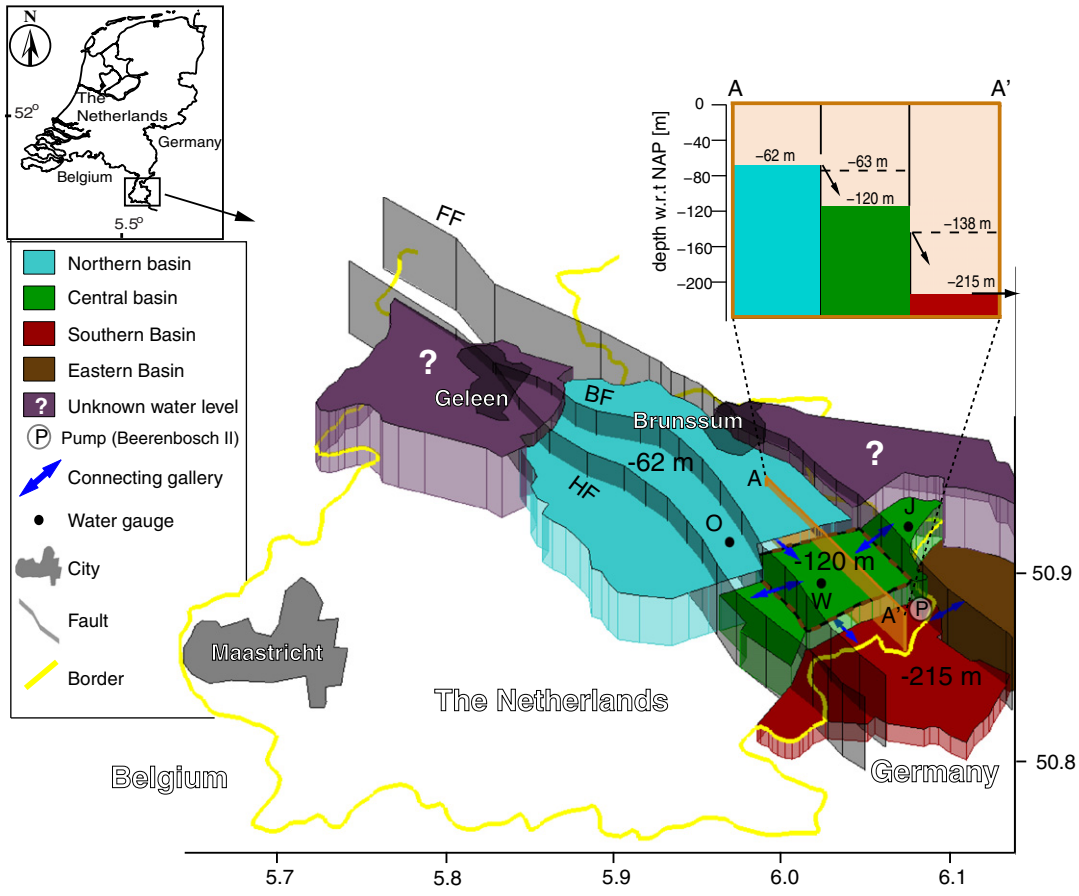

Fig. 2. The water basins in the Dutch and German coal regions with water levels as measured in 1994. The plotted vertical thickness indicates the water level whose value is indicated with respect to the vertical Dutch datum 'NAP', modified after Heitfeld et al. (2007). The profile A–A′ shows the hydraulic connections between the northern, the central and southern water basins, modified after Bekendam & Pöttgens (1995). The basin west of the northern basin is termed the Geleen-basin.

times can be both described with the same model plus a vertical offset to compensate for the displacement that occurs between the two reference images (one from ERS1/2 and the other from Envisat). The estimated vertical offset is added to Envisat observations to produced the joined time series. The error of this estimated offset (1σ) was ~4 mm or less for 95 % of PS.

2.1. Cumulative displacements

The total displacement field estimated by PSI for the period spanning from April 1992 to October 2009 is displayed in Fig. 3. The colored pixels represent those scatterers that are found to be coherent and selected as PS. They mostly relate to urban areas. The background picture is the corresponding time-averaged radar image. Estimated displacements are relative to a 1 km diameter area considered to be stable, centered at the village of Mechelen and displayed with a red circle in Fig. 3. To reduce the influence of a single scatterer, we average the displacements of the PS inside this area.

Total displacements are estimated by taking the differences of two periods assumed to represent the beginning and the end of the deformation signal. We average the measurements within the last period (June–October 2009) and compare it with the time span from April 1992 to December 1993.

To describe the quality of total displacements, we estimate their variance as well. The estimated variance is the sum of three terms: the variance of the displacement in the first period, the variance of the displacement in the last period and the $1-\sigma^2$ error of joining ERS1/2 and Envisat time series, (see above). As displayed in Fig. 4, the estimated standard deviation (equal to square root of the variance) is around 7 mm or less for 95% of PS, which is rather acceptable because total displacements are one order of magnitude larger for the mining areas.

Fig. 3 shows that most of the uplifting areas are within the coal field. Displacements are also bounded by faults, in some places, e.g., in Geleen and Brunssum [2] rather abruptly. This occurs when faults act as hydrological barrier, or when faults separate units with significantly different material properties, e.g., aquifers may not be found at the same depth at both sides of the fault.

The profiles shown in Fig. 5 explore the influence of the faults on the displacement field. Note the data gaps in 1994, as a consequence of an orbital change in ERS1, and from 2001 to 2004, which was the time interval between a malfunctioning of ERS2 gyroscopes and the start of systematic data acquisition by Envisat.

In the cities of Geleen and Brunssum, the gradients are 135 mm and 90 mm over a distance of 2.5 km and 1.6 km, respectively, in 18 years. In addition to that, the north of Brunssum is subsiding during the initial years of the time series, probably due to the influence of the open pit mines in Germany, where large amounts of water are pumped out (Bense et al., 2003). Further to the east of Brunssum and outside the area observed with InSAR there are three major lignite mines, see Fig. 1. After 2004, the situation in the north of Brunssum seems stable, which is consistent with the time series described in Section 2.2. In 2001, an earthquake swarm of low magnitude (from 1.5 to 3.9) was measured in the surroundings of Kunrade (KNMI, 2010). There were no clear indications that the motion was induced

[2] The mine concessions of Maurits and Oranje-Nassau correspond to the cities of Geleen and Brunssum.

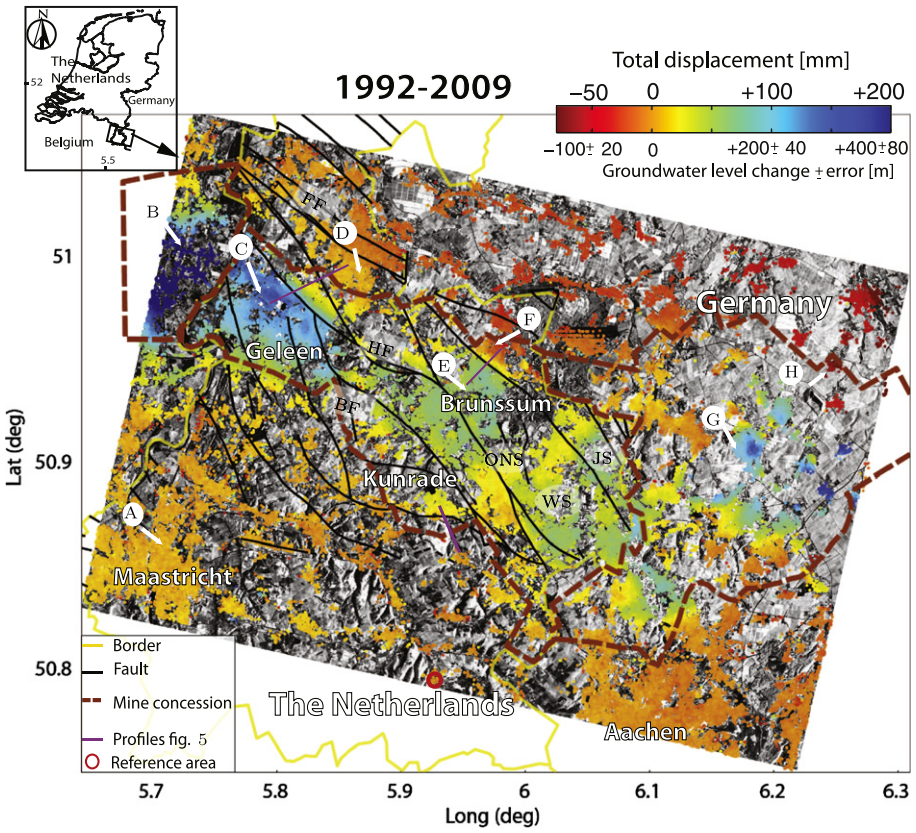

Fig. 3. Vertical cumulative displacement from 1992 to 2009 and estimated groundwater level change assuming constant skeletal coefficient and same thickness for the water basins (see text for explanation). A–H show location of Fig. 6. ONS (Oranje Nassau Shaft), JS (Julia shaft) and WS (Wilhelmina shaft) indicate the location of the places where the water gauges are placed installed. FF, HF and BF show the Feldbiss, Heerlerheide and Benzenrade faults, respectively.

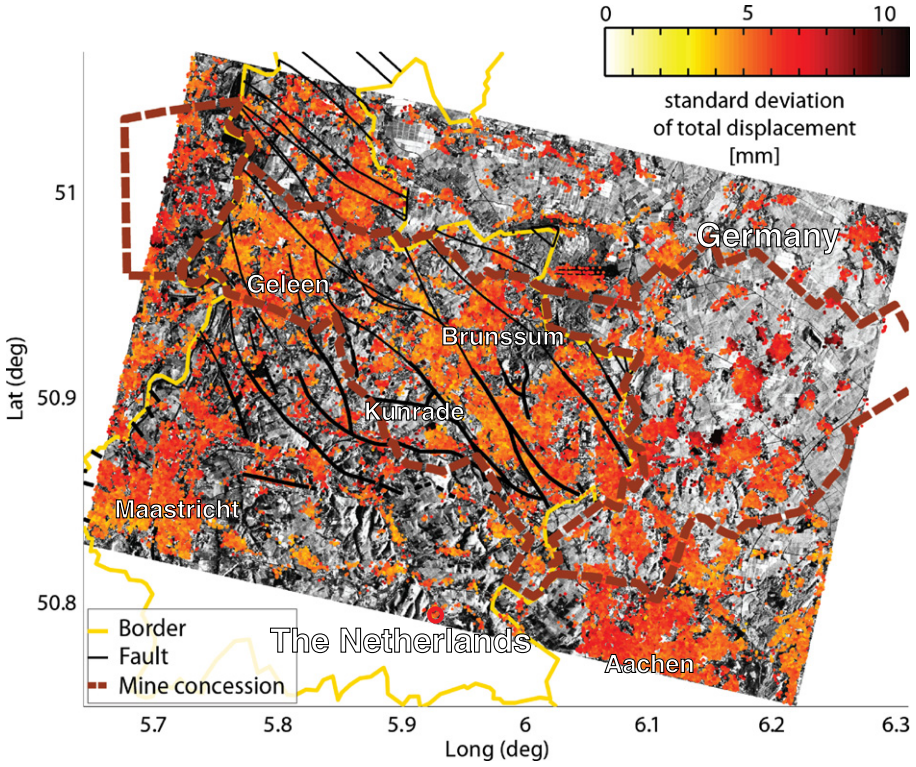

Fig. 4. Estimated standard deviation [mm] of cumulative displacements shown in Fig. 3 (1992–2009). In the precision estimation, we take into account the variability of the signal within each period (~5 mm for most PS) and the1 − σ error of joining ERS1/2 and Envisat time series (~4 mm).

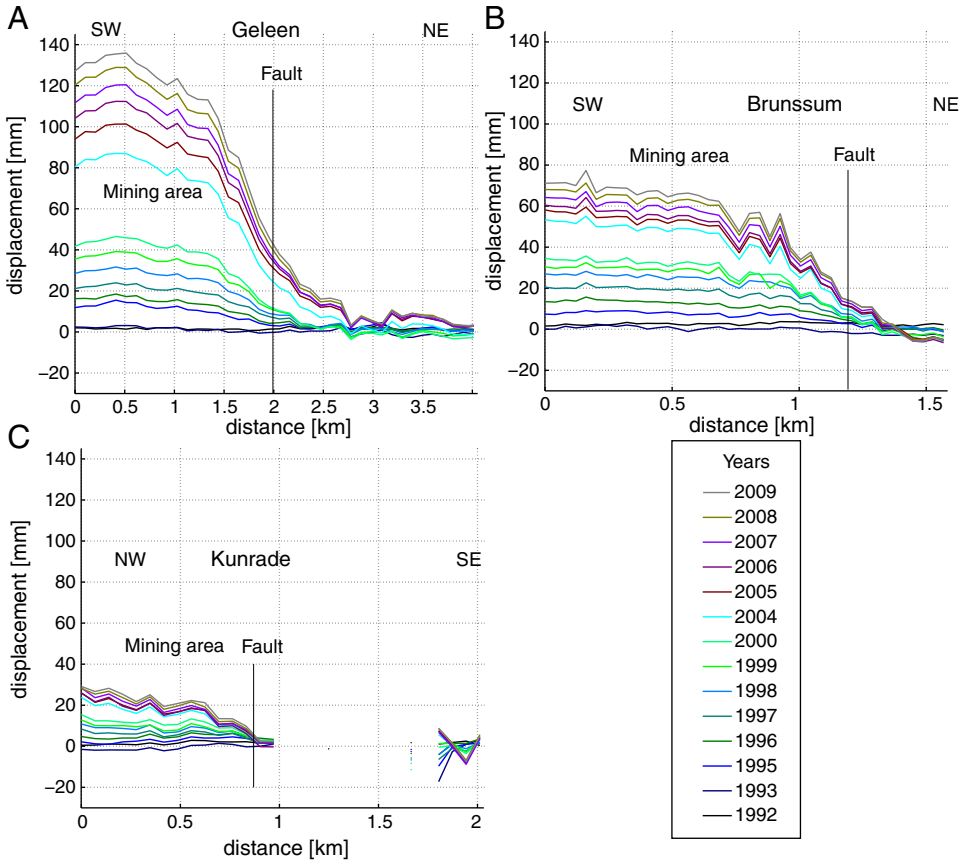

Fig. 5. Profile across the faults in the cities of Geleen (A) Brunssum (B) and Kunrade (C), showing yearly average deformation. The annual average is plotted. There are two data gaps in 1994 and from 2001 to 2004, (see text for explanation).

or related to the former mining activities. As can be seen from Fig. 5C, the uplift in the mining area is relatively moderate compared with the other two profiles. The influence of the fault is still visible; however, we do not detect any significant change in the ground displacements around the year of the earthquake swarm (2001). There are no apparent stable areas within the limits of the Dutch concessions, minimum values of the uplift signal are around +20 mm. The maximum is registered in Geleen with values around +135 mm, equivalent to ~8 mm/year. Outside this area, in the Belgian coal field, the uplift reaches values of about +220 mm. In this case, mine water pumping ceased during the early nineties (Devleeschouwer et al., 2008).

In Germany, we find two distinct motions with opposite behavior. In the northeast of Fig. 3, the land subsides due to the influence of open pit mines, for the same reasons as in north Brunssum. On the other hand, the area north of Aachen shows a total cumulative displacement of around +75 mm. Again, this corresponds to abandoned coal mines, which closed in 1992 (Heitfeld et al., 2002).

2.2. Time series

Eight locations are selected to provide an overview of the displacements in the studied area. The corresponding time series are plotted in Fig. 6. They were filtered in time and space to reduce noise.[3] ERS1/2 and Envisat time series are merged assuming that deformation signals can be described in time with a third degree polynomial plus a break point in 1994. The estimated standard deviation of an observation (PS displacements at a given time) is in the order of 5 mm plus the bias error of joining time series (~4 mm), which only affects the Envisat period. The locations of the time series are shown in Fig. 3 by the letters A to H. Note that during 1994 and from 2001 to 2004 there were no acquisitions.

As expected, the selected time series show that the most stable areas are located outside the coal fields. The city of Maastricht (time series 6A) appears stable when compared with the mining areas. As discussed in Section 1, the central and eastern side of the mine field experience the greatest cumulative uplift. Time series 6B, C and E show estimated ground displacements of these areas. They correspond to the mine concessions of Eisden in Belgium, Maurits and Oranje-Nassau in the Netherlands (see, e.g., TNO (1999), van Tongeren and Dreesen (2004)). Time series 6B is located in the Belgian coal field and is not in hydrologic connection with the Dutch mines. From 1992 to 1994, time series 6B is stable, which is in agreement with the fact that the Belgian water pumps were still active until the early nineties (Devleeschouwer et al., 2008). After that the deformation accelerates very fast. The area uplifts during the whole study period. Time series 6C and E show the land deformation of the mine concessions in Geleen and Brunssum, respectively. The time series show stability until 1995, then an initial slow uplifting signal that accelerates around 1997 and 1998 in Brunssum and Geleen, respectively. After the acceleration, the surface starts to uplift almost linearly with time. The acceleration is probably caused by water overflowing between basins. We explore further the hydraulic connection between Geleen and Brunssum areas and the pump in Beerenbosch II in Section 3. The effect of the only remaining pump (see location in Fig. 2), which was 10 km from Brunssum (E) and 25 km from Geleen (C) still visible in the time series, suggesting that water pumping influences over large distances.

[3] In the time filter, we employed a moving average with a Gaussian window of 4 months. The filter in space was performed with kriging with an exponential variogram that had a range of ~300 m.

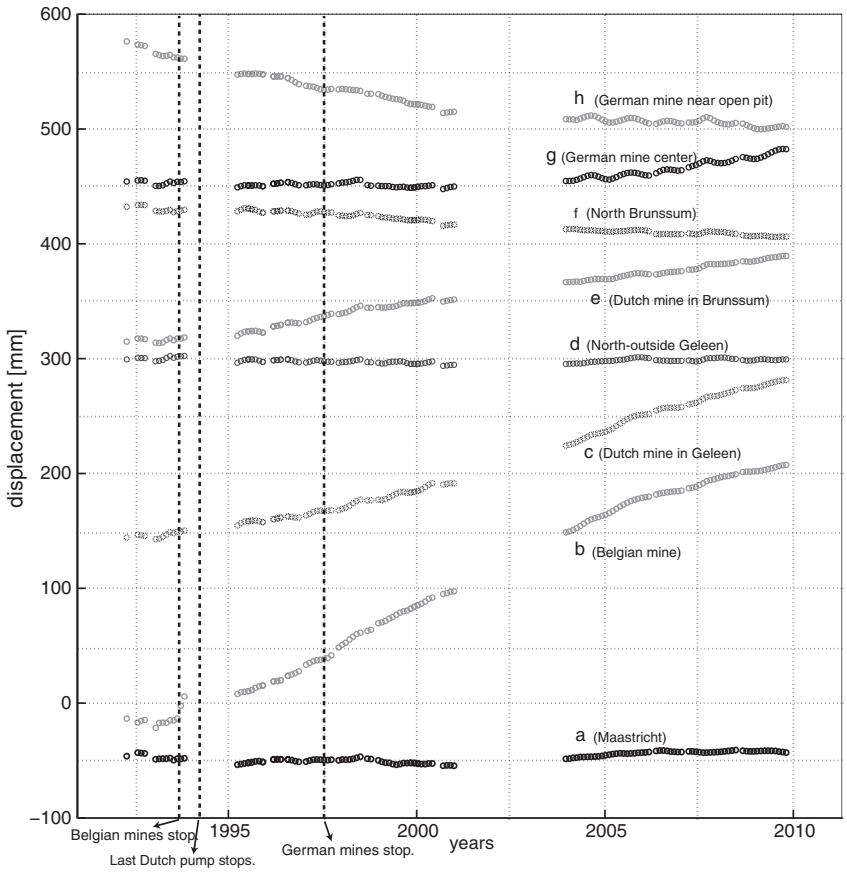

Fig. 6. Deformation time series at eight places relative to the reference area. See location in Fig. 3 from the letters A to H. Vertical offsets are added for visualization. The estimated standard deviation of the observations are in the order of 5 mm plus the $1-\sigma$ error of joining time series (~4 mm). Error bars are not displayed in Fig. 6 due to the large scale.

From series 6D and F, we see that PS located outside the concession area and separated from the mining area by tectonic faults are not affected by the uplift, see also Fig. 5.

Time series 6G is located in the German mining area. Here, the coal extraction stopped in 1992 (Heitfeld et al., 2002), but uplift started only after 2001. Presumably, this is because a possible water rebound is compensated by the subsidence caused by water pumping in other mines (the open pit mines) along with the residual subsidence from the mining, i.e. a delayed reaction to the extraction, see e.g. (Blodgett and Kuipers, 2002). Water induced uplift seemed to have taken over in 2004 when this area started to heave.

Time series 6 H reflects the influence of water extraction required for the operation of the open pit lignite mine located outside the radar images and to the north-east of Aachen. The subsidence rate in Fig. 6H decreased with time from around −10 mm/year before 2001 to −1 mm/year after 2004. This suggests that the pumping rate in the open pit mines decreased during this period.

Some of the time series display a periodic annual signal. This is visible in series 6G and H in particular after 2004. Periodic signals are produced by effects such as surface water variations due to seasonal evaporation and recharge or temperature changes (see e.g. Crosetto et al. (2011), van Leijen and Hanssen (2008) or Caro Cuenca and Hanssen (2008)). The amplitude of the periodic signal does not only depend on the geophysical properties of the signal itself but also on the scattering object (PS). For example, an object with deep foundations (e.g., a tall building) will not be influenced by shallow seasonal motions. This is probably the cause of the differences between the periodic signal observed by Envisat (after 2004) and ERS1/2 (before 2001). The PS detected by one satellite are usually not the same as detected by another due to changes in terrain with time and differences in the viewing angle. As described above, the time series were joined by spatially interpolating Envisat observations to the locations of PS detected by ERS1/2.

In summary, time series derived from PSI observations show that the areas located within the bounds of the mine concessions are under the influence of mine water recharge after pumping ceased. Furthermore, the water extraction at German open pit mines, located to the east of the study area, also affects the displacement field producing subsidence. On the other hand, time series located outside the mine limits appear to be stable.

3. Spatio-temporal evolution of mine water recharge from surface displacements

The satellite results suggest that there may be a causality between the cessation of pumping and the surface uplift. In this section, we propose a rough functional relationship between surface deformation from PS time series and hydraulic heads (groundwater levels) measured at the mine depth, evaluated at the only three locations where this information is available. Under the assumption that the validity of the model can be laterally extended, this enables a first estimation of hydraulic heads elsewhere in the region, where such information is not available from other sources.

3.1. Groundwater levels

Fig. 7 displays the groundwater levels and the corresponding displacements at three shafts: Julia (JS) and Wilhelmina (WS) in the central basin, and Oranje Nassau (ONS) in the northern basin, see Figs. 3 and 2. The right vertical axis (water level) is scaled based on

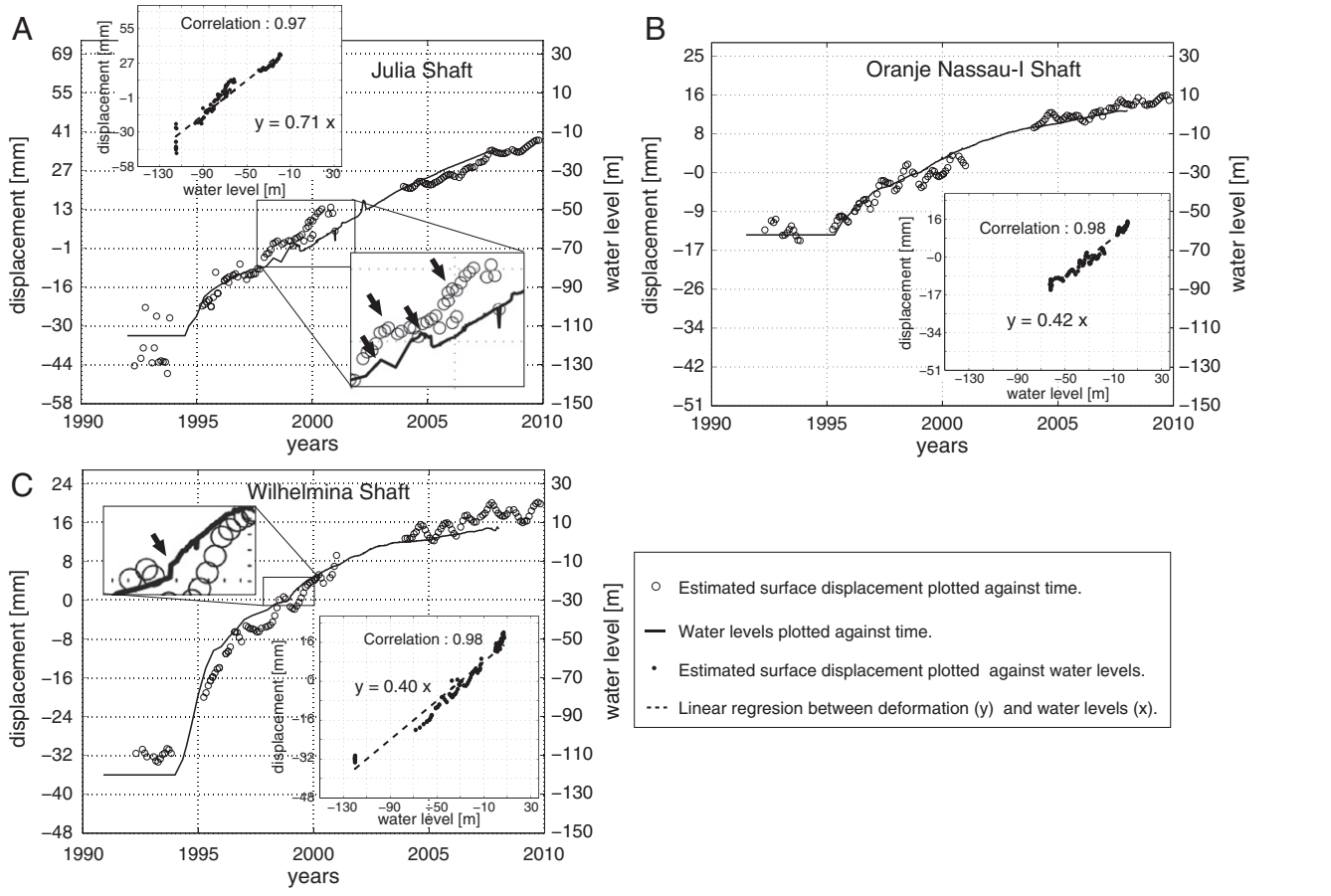

Fig. 7. Surface displacements and water levels at A) Julia shaft, B) Oranje Nassau-I Shaft, and C) Wilhelmina shaft. Their locations are indicated in Fig. 3 with JS, ONS and WS respectively. Water levels are with respect to NAP. The ups and downs of the water level at Julia shaft are due to pumping tests, marked with black arrows. This is also visible in the Wilhelmina shaft but very slightly showed also as a zoom in and marked with black arrow. The estimated standard deviation of an observation (PS displacements in a given time) is in the order of 5 mm plus the $1-\sigma$ error of joining time series (~4 mm), which only affects Envisat observations. Error bars are not shown in the figure for simplicity.

a linear regression between surface displacements and water levels. The results show that groundwater levels were constant before 1994. In this year, the pump in Beerenbosch II was dismantled and the groundwater levels started to rise. The small variations of the water level in the Julia shaft, indicated by the arrows in Fig. 7A, resulted from pumping tests (Heitfeld, personal communication, 2008). This is also visible, albeit very slightly, in the water levels at Wilhelmina, see the arrow in the zoom-in of Fig. 7C. In the Julia shaft, surface displacements seem to react to water level changes with some months delay, as displayed in the zoom-in of Fig. 7A.

In all cases, the groundwater levels show a very high correlation (~0.97) with surface displacements, see the inset plots in Fig. 7. The only exception is found for the data of the Julia shaft, for dates prior to 1994, see Fig. 7A, probably due to noise and decreased coherence, leading to uncertainties in the phase ambiguity resolution (Hanssen, 2001). Apart from the major signal related to mine water, the time series also show periodic variation, clearly visible in Fig. 7B and C. This is probably caused by seasonal phenomena at much shallower depths, e.g. variation in the vadose zone, unrelated to the deep mine water recharge.

The inset plots of Fig. 7 show an almost linear relationship between displacements obtained by PSI and the water levels. From this, we can estimate the storage coefficient S_{ke} for the central and northern basin. The elastic skeletal storage coefficient S_{ke} (or simply, storage coefficient) gives very valuable information on the response of the (fractured) rock to pore pressure changes. This coefficient, usually employed in the analysis of confined aquifers, gives a first approximation of the relationship between water level changes and rock dilatation (Hoffmann, 2003). Groundwater levels in the mines are not in direct contact with the phreatic surface (Rosner, 2011; van Bracht, 2001), i.e. this system can be assumed to be confined. It is evident that saturated conditions may not be fully met as we deal with an underground mining site with open or collapsed galleries. Nevertheless, as more detailed information on the mines is lacking, estimating a storage coefficient can be the only option to improve our knowledge on the response of the mined ground to pore pressure increase.

When small changes in the effective stress happen, caused by changes in hydraulic heads, this leads to a linear relationship with vertical surface deformation (Hoffmann, 2003),

$$S_{ke} \approx \frac{\Delta z}{\Delta h_w}, \tag{1}$$

where the storage coefficient S_{ke} expresses the vertical expansion of the rock Δz for a certain head (groundwater level) change Δh_w. Assuming that the vertical changes of the disturbed rock are equal to the displacements observed at the surface, (Hoffmann, 2003), we estimate S_{ke} to be $(0.71 \pm 0.05)\ 10^{-3}$ and $(0.40 \pm 0.05)\ 10^{-3}$ for the shafts of the Julia and Wilhelmina mines, respectively, both in the central basin. In the south of the northern basin, we estimate for the Oranje–Nassau I shaft a value of $S_{ke} = (0.42 \pm 0.05) \cdot 10^{-3}$. These estimates imply roughly that a 10 m increase in mine water level will result in surface uplifts of around 7.1 mm, 4.2 mm, and 4.0 mm, for the three mines, respectively. The locations of the three shafts with available hydraulic head records are all confined to only the eastern side of the entire Limburg mining region. Therefore, there is a serious

lack of groundwater records for most of the mining areas. Assuming that the three estimated storage coefficients are indicative for the rest of the mining area, we use the average overall storage coefficient of $\bar{S}_{ke} = 0.5 \pm 0.1 \cdot 10^{-3}$. With this approximation, we estimate the groundwater level changes that occurred from 1992 to 2009 from the observed displacements using Eq. (1). These values are displayed in Fig. 3, using the same colorbar for cumulative displacements. These results show, for example, that the ground water level in the Geleen-basin rose 250 ± 50 m in this period.

Apart from estimating geophysical properties of the mined rock, the comparison between groundwater and surface displacements also reveals that the chronology of events related to groundwater levels is reflected by PS estimations. In the shafts of Wilhelmina and Julia the groundwater levels started to rise almost simultaneously with the cease of water pumping (1994), and so does the corresponding surface displacement. In the shaft of Oranje-Nassau I, the groundwater levels took a year longer to start rising, also confirmed by the onset of the observed surface uplift in 1995. In the following, we discuss the evolution of groundwater influx from the observed spatio-temporal surface displacements.

3.2. Analysis of spatio-temporal water recharge

To study the spatio-temporal evolution of mine water recharge in the Dutch coal field, we draw a profile of yearly cumulative displacements. The results, see Fig. 8, show the total surface displacement from the beginning of the time series (April 1992) to the indicated year. The profile is drawn between Geleen (A) and Beerenbosch II (A′) and crosses the whole Dutch coal field, see the location in Fig. 8. The overall dynamics suggest the mine water to propagate from the southeast to the northwest. From the southern basin, which is where the pump was located (see location in Fig. 2), the uplift propagates towards the central basin and from here towards the northern basin and the mining area of Geleen, suggesting the same flow direction for the groundwater.

From the temporal evolution, we observe that the ground appears relatively stable in the whole Dutch coal field for the first years (1992–1993). Then, in 1994, when the pump in Beerenbosch II is dismantled, the surface quickly rises in the southern basin. Soon after, the water 'overflows' to Wilhelmina. Effectively, the difference in surface displacement between the Wilhelmina Shaft and Beerenbosch II suggests that the overflowing towards the central basin is not immediate after cessation of pumping. This is also confirmed with the time series discussed in Section 3.1.

The moderate displacement signal that we observe in the northern basin before 1996 indicates that the water level in this basin is increasing very slowly compared with, e.g., Beerenbosch II. This can be explained if the water in the central basin has not reached an overflowing gallery connecting this with the northern basin. Therefore the conductivity between these two basins is, until now, low.

In 1996, we observe an acceleration in the displacements in the central basin that suggests that water is overflowing from the southern basin in this year. High deformation rates are maintained in this basin until 1999, whereafter rates decay with time. On the other hand, the acceleration of the uplift in the mine under Geleen appears in 1998, which probably indicates the time when water overflows from the northern basin.

Comparing the temporal evolution of the basins, we see that surface displacements in the central and southern basins have almost halted at the end of our time series. In the northern basin and the area of Geleen the surface continues to uplift. This suggests that while water level increase in the central and southern basins is now very low, in the northern basins and the Geleen area the water is still rising. This could be related to the natural slope of the carboniferous layers. The depth of this layer increases from east to west (TNO, 1999), which could make the water flow in the observed direction.

Interestingly, the annual cumulative deformations depicted in Fig. 8 reveal that the confinements of the hydrological units (associated with NE-SW oriented faults) experience very modest uplift rates, less than ~25 mm, or 2–5 times less than the centers of the hydrological units. Geographically, these areas with relatively low uplift rates are situated around Schinnen, between Heerlerheide and Heerlen-north, and around Spekholzerheide. Along the profile of Fig. 8 this corresponds with distances of 7.5, 16–17, and 22.5 km from the western side of the profile, respectively. It is important to stress that the areas situated directly east and west of these three locations experience the highest relative spatial gradients in uplift velocities, and are therefore probably most susceptible for infrastructural damage at the surface.

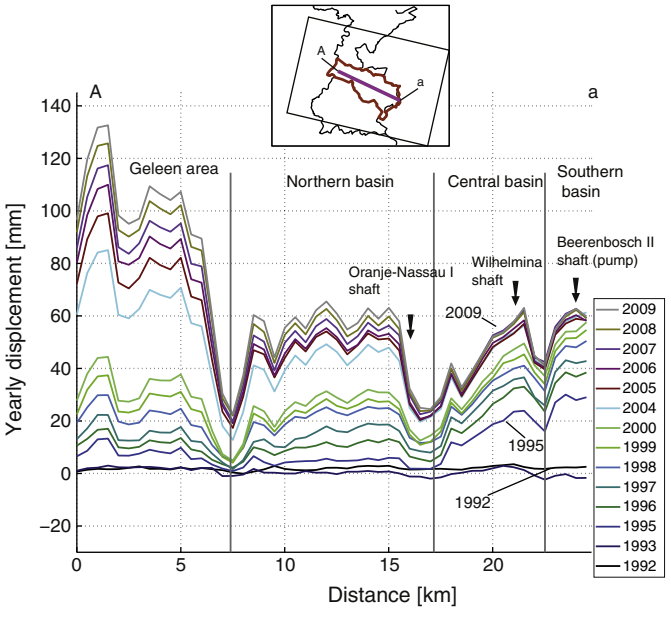

Fig. 8. Profile of the annual cumulative deformation across the whole Dutch coal field, from Geleen to Beerenbosch II. There are two data gaps in 1994 and from 2001 to 2004, (see text for explanation).

4. Modeling the underground volume change

Here we present the model used to estimate volume change in the Limburg mines, followed by the results of the inversion from the observed displacements.

4.1. Strain source theory

To study volume change due to pore pressure variations, we apply the strain source concept.[4] This was first introduced by Geertsma (1973) to explain the relationship between gas reservoir compaction and surface subsidence, assuming a uniform elastic half-space. Geertsma's method was developed independently, but is similar to earlier approaches by Anderson (1936) and (Mogi, (1958). The shape of the reservoir is modeled with a homogeneous grid of strain sources and integrating them spatially. Pöttgens (1985) employed strain sources to study surface uplift in the Dutch coal mines, suggesting that the rising waters produced an increase of pore pressure in the disturbed rock. The consequent rock volume increase translated into surface uplift. During coal extraction, the porosity the rock is increased considerably, making the rock prone to ingress water (Bekendam and Pöttgens, 1995; Pöttgens, 1985).

[4] The term *nucleus of strain* (Geertsma, 1973) is here renamed as *strain source*.

Geertsma (1973) proposed that the vertical displacement, u_z, produced by a strain source of small but finite volume V at depth D due to pore pressure change Δp, can be calculated from

$$u_z(R, z=0) = -\frac{1}{\pi} d_m (1-\nu) \frac{D}{(R^2+D^2)^{\frac{3}{2}}} \Delta p V, \tag{2}$$

where R is the radial distance to the strain source, $z=0$ corresponds to the ground level surface, and ν is Poisson's ratio. The z-axis is defined positive in the up-direction, implying that the depth D has a negative value. The term d_m is the uniaxial dilatation coefficient, originally defined by Geertsma and van Opstal (1973) as 'uniaxial compression coefficient' but renamed by Pöttgens (1985). This is given by

$$d_m = \frac{1}{Z} \frac{dz}{dp}, \tag{3}$$

where p is the pressure and Z is the initial vertical extent of the strain source volume. Note that the uniaxial compression coefficient defined by Geertsma and van Opstal (1973) is equivalent to the definition of the storage coefficient S_{ke} given in Eq. (1). Assuming an elastic half-space, volume increase primarily occurs in the vertical dimension, so Eq. (3) can be rephrased as

$$d_m = \frac{1}{V} \frac{\Delta V}{\Delta p}, \tag{4}$$

where V is the volume of the reservoir equal to the assumed fixed horizontal extension, A, of the reservoir times the vertical dimension Z. Thus, Eq. (2) can be rephrased as

$$u_z(R, z=0) = -\frac{1}{\pi} (1-\nu) \frac{D}{(R^2+D^2)^{\frac{3}{2}}} \Delta V, \tag{5}$$

where ΔV is the volume change of the strain source.

The total vertical deformation at the surface produced by a homogeneous grid of strain sources is calculated by summing the contribution of each source (Geertsma and van Opstal, 1973). We model the volume change due to pore pressure variations with a uniform grid of closely spaced strain sources. Since water recharge is the cause of the deformation, the strain source depth is taken to be at the water levels with respect to surface, −250 m (Bekendam and Pöttgens, 1995).

To prevent a solution that is physically impossible, we constrain the sources spatially. We assume that the strain sources form disk-shaped hydrological units (Geertsma, 1973; Pöttgens, 1985). To estimate the characteristic radius of the disks, r_c, we employ a pressure distribution found for water extraction in reservoirs (Segall et al., 1994). In this case, an exponential decline of the pressure p with distance r with respect to a drainage point is assumed:

$$p(r,t) = p_0(t) e^{-(r/r_c)^4}, \tag{6}$$

where t is the time, $p_0(t)$ is the maximum pressure change at $r=0$, and r_c is the characteristic radius of the reservoir, which defines the main area of influence of the pumping.

We assume that the same expression is also valid for the inverse situation — when pore pressure increases. The pressure increase is then maximum at the location of the pump, and decaying exponentially with distance as in Eq. (6). We can also find the distribution of volume change with Eqs. (4) and (6):

$$\Delta V(r) = V d_m \Delta p = V d_m (p_0(t_2) - p_0(t_1)) e^{-(r/r_c)^4} = \Delta V_0 e^{-(r/r_c)^4}, \tag{7}$$

where ΔV_0 is the maximum volume change. Essentially, this is equivalent to model the hydrological units as disk-shaped reservoirs of radius r_c.

Since the coal field has different overflowing galleries connecting the water basins, we assume that the distribution of volume change given in Eq. (7) can happen at different places in the coal field. Therefore, we also estimate the numberof disk-shaped reservoirs needed to model the coal field.

4.2. Modeling rock dilatation

To model volume increase of the rocks of the Dutch mines, we combine Eqs. (5) and (7). For the Poisson's ratio we employ the value $\nu = 0.25$ suggested by Bekendam and Pöttgens (1995). To estimate the required number of disk-shaped reservoirs, we first perform an automated search for the location of local maxima in the displacement field.

For the Dutch mines, this yields ten local maxima whose locations are displayed in Fig. 9 as black circles. We model the volume increase experienced by the mined ground as being equivalent to ten disk-shaped units with increasing pore pressure. The disk size and location

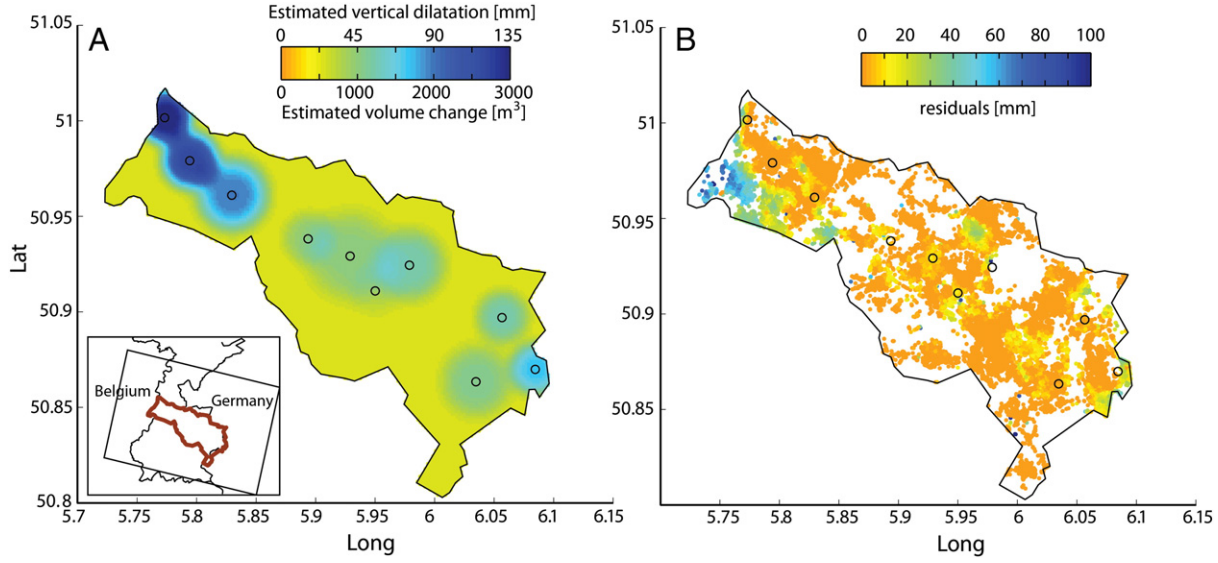

Fig. 9. A) Modeled volume change caused by pore pressure increase. Estimated vertical dilatation is also displayed and calculated assuming the dilatation is only vertical. B) Residuals obtained after subtracting measured to modeled deformation. The black circles show the location of a local maxima which are used in the model (see text for explanation).

are estimated from the data regardless of the real location of previously active pumps. This means that, although the model fairly represents the volume increase experienced by the mined ground, the disk-shaped units do not necessarily reflect the actual geophysical situation.

The unknowns to be estimated are the maximum volume change, ΔV_0, and the characteristic radius, r_c, per local maxima, yielding 20 unknowns in total. Since Eq. (7) is non-linear, a search in the parameter space of r_c is performed. The estimated volume increase is displayed in Fig. 9A and the residuals (observed minus modeled displacements) in Fig. 9B. From the residuals we observe a fair fit of the model for most of the areas with the exception of the western lower corner of the Dutch concessions.

The predicted vertical dilatation $\Delta\hat{z}$ is calculated for a uniform grid of volume elements with a posting of $S = 150$ m, based on the ten initial disks, using the estimated volume increase $\Delta\hat{V}$, assuming this is only in the vertical direction:

$$\Delta\hat{z} = \frac{\Delta\hat{V}}{S^2}. \tag{8}$$

The estimations show that the places with greatest volume change are concentrated in three different areas revealing the mines which may have the highest storage coefficients. As discussed in Section 3, the areas with relatively low vertical uplift (~25 mm) were probably not affected by the coal extraction process (due to the faults). Maximum values of volume increase are found in the western mines, corresponding to the area of Geleen. In this area the vertical dilatation reaches around 135 mm. This can be explained either by a higher dilatation coefficient or by a greater increase in pressure, caused by the increased influx of water in this part of the region. Since there is a temporal pattern in the rising of water levels in the different hydrological units, it is more likely that the observed higher uplift rates in the west, for the latest periods, are caused by an increased water flux in the region at those times.

5. Discussion and conclusions

Surface displacements observed by satellite radar interferometry show unambiguously that most of the abandoned coal fields in the southern Netherlands, Germany and Belgium were rising during the period 1992–2009. Displacements of up to +220 mm in 18 years are measured for the mines in Belgium. In the Netherlands a maximum of +125 mm is found in the Dutch western mining area, near Geleen, over the same period. The uplift signal is highly variable in space and time. Spatially, the uplift is strictly confined to areas bounded by faults, both the major NW–SE trending faults parallel to the Roer-Valley Graben, as well as faults orthogonal to this system. Temporally, the uplift rate is initially (1992–1995) greatest in the south-eastern mining area, but around 1999–2004 the process progresses towards the north-western mining areas. Comparing observed surface displacements with mine water levels at three old shafts in the east of the mining area shows that there is a strong correlation. Assuming comparable situations in the entire region, we estimate an average storage coefficient of $0.5 \pm 0.1\ 10^{-3}$, implying that 10 m water level increase results in 0.5 cm of surface uplift. Under these assumptions, we estimated that for the area of Geleen, where the groundwater cannot be directly measured, the groundwater level has risen around 250 ± 50 m from 1992 to 2009. The time series in Geleen suggest that the groundwater is currently still rising.

The temporal progression of the surface uplift suggests complex sub-surface water dynamics. In 1995 the rising water in the southern basin reached the overflowing gallery, connecting it to the central basin, and in 1996 the water reached the northern basin. The PSI displacements show that the water from the northern basin started to overflow towards the Geleen-basin in 1998, when we observe an acceleration in the motion.

A simple model based on a distribution of strain sources and an inverse exponential pressure decline allows for the estimation of volume change based on the surface measures. Pressure and volume changes are indicative for an increased influx of water in a confined basin.

The influence of tectonic faults in the displacement field is clearly visible in the deformation data due to the strong gradients orthogonal to the faults. Apparently, the faults act as hydrological barriers, preventing water to flow freely across a fault. This could be due to the decrease in permeability of the fault zone, perhaps caused by a grinding effect associated with motion along the fault. Alternatively, it could be due to the stratigraphic differences on both sides of the fault, where less permeable strata on one side are situated next to more permeable strata at the other side, causing differences in the behavior of propagating fluids. The strong gradients in uplift rates cause differential motion on relatively short (0.1–1 km) spatial scales. This may inflict strain on buildings and infrastructure. Although risk assessment is beyond the scope of this study it is worth noting that the results of our analysis identify several areas which seem prone to infrastructure damage.

6. Acknowledgments

We would like to thank The Netherlands' Research Centre for Integrated Solid Earth Science (ISES) for funding this research and the European Space Agency for providing satellite data via project Cat-4048. We are indebted to Hans Roest at the State Authority of Mines (SodM) for providing water level data and valuable discussions. We would like to thank Ingenieurbüro Heitfeld-Schetelig GmbH and Roland Bekendam and Roy Wings for giving us a better insight of mining engineering and for first reviews of this paper. We are especially grateful to Jan J. Pöttgens († 2009) for the fruitful discussions and all his experience and knowledge he shared with us.

References

Anderson, E.M., 1936. The dynamics of the formation of cone-sheets, ring-dykes, and caldron subsidence. Proceedings of the Royal Society of Edinburgh 56, 128–157.

Bekendam, R.F., Pöttgens, J.J., 1995. Ground movements over the coal mines in southern Limburg, The Netherlands and their relation to rising mine waters. In: Johnson, A.I. (Ed.), Proceedings of the fifth international symposium on land subsidence (FISOLS'95), The Hague, The Netherlands, 16–20 Oct 1995. Balkema, Rotterdam, pp. 3–12.

Bense, V.F., van Balen, R.T., de Vries, J.J., 2003. The impact of faults on the hydrogeological conditions in the Roer Valley Rift System: an overview. Netherlands Journal of Geosciences / Geologie en Mijnbouw 82 (1), 41–54.

Blodgett, S., Kuipers, J.R., 2002. Underground hard-rock mining: subsidence and hydrologic environmental impacts. Technical reportCenter for Science in Public Participation, Bozeman, MT, USA.

Caro Cuenca, M., Hanssen, R., 2008. Subsidence due to peat decomposition in the Netherlands, kinematic observations from radar interferometry. Fifth International Workshop on ERS/Envisat SAR Interferometry, 'FRINGE07', Frascati, Italy, 26 Nov-30 Nov 2007 (6 pp).

Caro Cuenca, M., Hanssen, R., 2010. A Least-square Approach for Joining Persistent Scatterer Insar Time Series Acquired by Different Satellites. Living Planet Symposium, Bergen, Norway . (28 June–2 July 2010, pp. 7 pp).

Caro Cuenca, M., Hanssen, R., 2011. Radar time series analysis applied to study surface motion in the abandoned coal mines of Wassenberg. Geophysical Monitoring 11.

Caro Cuenca, M., van Leijen, F., Hanssen, R., 2010. Shallow subsidence in the Dutch wetlands estimated by satellite radar interferometry. First International Conference on Frontiers in Shallow Subsurface Technology, Delft, the Netherlands, 20–22 January 2010 (4 pp).

Crosetto, M., Monserrat, O., Cuevas, M., Crippa, B., 2011. Spaceborne differential SAR interferometry: data analysis tools for deformation measurement. Remote Sensing 3 (2), 305–318.

Devleeschouwer, X., Declercq, P.Y., Dusar, M., Debien, A., 2008. Contrasting ground movements revealed by radar interferometry over abandoned coal mines (Campine, Belgium). Fifth International Workshop on ERS/Envisat SAR Interferometry, 'FRINGE07', Frascati, Italy, 26 Nov-30 Nov 2007 (8 pp).

Ferretti, A., Prati, C., Rocca, F., January 2001. Permanent scatterers in SAR interferometry. IEEE Transactions on Geoscience and Remote Sensing 1, 8–20.

Geertsma, J., 1973. A basic theory of subsidence due to reservoir compaction: the homogeneous case. Transactions of the Royal Geological and Mining Society of the Netherlands 28, 43–62.

Geertsma, J., van Opstal, G., 1973. A numerical technique for predicting subsidence above compacting reservoirs, based on the nucleus of strain concept. Transactions of the Royal Geological and Mining Society of the Netherlands 28, 63–78.
Hanssen, R.F., 2001. Radar Interferometry: Data Interpretation and Error Analysis. Kluwer Academic Publishers, Dordrecht.
Heitfeld, K.H., Heitfeld, M., Rosner, P., Sahl, H., Schetelig, K., 2002. Mine water recovery in the coal mining district of aachen â€“ impacts and measures to control potential risk. Uranium in the Aquatic Environment. Springer, Heidelberg, pp. 1027–1036.
Heitfeld, M., Mainz, M., Schetelig, M.M.H., 2006. Ground heave induced by mine water recovery. Eurock 2006: multiphysics coupling and long term behaviour in rock mechanics, pp. 315–320.
Heitfeld, M., Rosner, P., Boger, J., 2007. Technical report, IngenieurbÃ¼ro Heitfeld-Schetelig GmbH (IHS).
Heitfeld, M., 2008. Personal communication.
Hoffmann, J. (2003). *The application of satellite radar interferometry to the study of land subsidence over developped aquifer systems*. Ph. D. thesis, Stanford University.
Hooper, A., Zebker, H., Segall, P., Kampes, B., December 2004. A new method for measuring deformation on volcanoes and other non-urban areas using InSAR persistent scatterers. Geophysical Research Letters 31, L23611 http://dx.doi.org/10.1029/2004GL021737.
Kampes, B.M., 2006. Radar interferometry: persistent scatterer technique. Remote Sensing and Digital Image Processing, 12. Dordrecht, Springer Verlag.
Kampes, B.M., Hanssen, R.F., Perski, Z., 2003. Radar interferometry with public domain tools. Third International Workshop on ERS SAR Interferometry, 'FRINGE03', Frascati, Italy, 1–5 Dec 2003 (6 pp).
KNMI, May 2010. Aardbevingen bij voerendaal en kunrade (2001).
Mogi, K., 1958. Relations between eruptions of various volcanoes and the deformations of the ground surfaces around them. Bulletin of the Earthquake Research Institute-University of Tokyo 36, 99–134.
Pöttgens, J.J.E., 1985. Bodemhebung durch ansteigendes Grubenwasser [Uplift as a result of rising mine waters]. The Development Science and Art of Minerals Surveying, Proceedings VIth International Congress: International Society for Mine Surveying, Harrogate, United Kingdom, 9–13 September 1985, 2, pp. 928–938.
Pöttgens, J.J.E., 2008. Personal communication.
Rosner, P. (2011). *Der Grubenwasseranstieg im Aachener und SÃ¼dlimburger Steinkohlenrevier. Eine hydrogeologisch-bergbauliche Analyse der WirkungszusammenhÃ¤nge*. Ph. D. thesis, Germany.
Scharroo, R., Visser, P., 1998. Precise orbit determination and gravity field improvement for the ERS satellites. Journal of Geophysical Research 103 (C4), 8113–8127.
Segall, P., Grasso, J.-R., Mossop, A., 1994. Poroelastic stressing and induced seismicity near Lacq gas field, southwestern France. Journal of Geophysical Research 99 (B8), 15423–15438.
TNO, 1999. Geological Atlas of the Subsurface of The Netherlands, Map Sheet XV, Sittard-Maastricht,Netherlands Institute of Applied Science. National Geological Survey, Utrecht: TNO.
van Bergen, F., Pagnier, H.J.M., van Tongeren, P.C.H., 2007. Peat, coal and coalbed methane. In: Wong, T.E., Batjes, D.A.J., de Jager, J. (Eds.), Geology of the Netherlands. Royal Netherlands Academy of Arts and Sciences, Amsterdam, pp. 265–282.
van Bracht, M. J. (2001, May). *Made to measure: Information requirements and groundwater level monitoring networks*. Ph. D. thesis, Vrije Universiteit Amsterdam, Amsterdam, The Netherlands.
van Leijen, F., Hanssen, R., 2008. Ground water management and its consequences in Delft, the Netherlands as observed by persistent scatterer interferometry. Fifth International Workshop on ERS/Envisat SAR Interferometry, 'FRINGE07', Frascati, Italy, 26 Nov-30 Nov 2007 (6 pp).
van Tongeren, P.C.H., Dreesen, R., 2004. Residual space volumes in abandoned coal mines of the Belgian Campine basin and possibilities for use. Geologica Belgica 7 (3–4), 157–164.
Wings, R., 2006. A review of ground movements over abandoned coal mines in Limburg, the Netherlands. Ingeokring Newsletter 13 (1), 6–9.
Wings, R., 2011. Personal communication.